Naval Research Laboratory
Washington, DC 20375-5320

NRL/5310/MR—2023/2

Analysis of Bulk Dielectric Constant of Latticed Materials

ANNA STUMME

MARK DORSEY

Radar Analysis Branch
Radar Division

ALEXANDER GOLDING

Mechanical Engineering and Fabrication Section
Tactical Electronic Warfare Division

SCOTT RUDOLPH

Airborne Electronic Payloads Research Section
Tactical Electronic Warfare Division

April 17, 2023

REPORT DOCUMENTATION PAGE

Form Approved
OMB No. 0704-0188

1. REPORT DATE *(DD-MM-YYYY)*	**2. REPORT TYPE**	**3. DATES COVERED** *(From - To)*
17-04-2023	NRL Memorandum Report	2021 – 2023

4. TITLE AND SUBTITLE

Analysis of Bulk Dielectric Constant of Latticed Materials

5a. CONTRACT NUMBER

5b. GRANT NUMBER

5c. PROGRAM ELEMENT NUMBER
62271N

6. AUTHOR(S)

Anna M. Stumme, Mark W. Dorsey, Alexander Golding, and Scott Rudolph

5d. PROJECT NUMBER

5e. TASK NUMBER

5f. WORK UNIT NUMBER
6C78

7. PERFORMING ORGANIZATION NAME(S) AND ADDRESS(ES)

Naval Research Laboratory
4555 Overlook Avenue, SW
Washington, DC 20375-5320

8. PERFORMING ORGANIZATION REPORT NUMBER

NRL/5310/MR--2023/2

9. SPONSORING / MONITORING AGENCY NAME(S) AND ADDRESS(ES)

Naval Research Laboratory
4555 Overlook Avenue, SW
Washington, DC 20375-532

10. SPONSOR / MONITOR'S ACRONYM(S)

NRL Base Program

11. SPONSOR / MONITOR'S REPORT NUMBER(S)

12. DISTRIBUTION / AVAILABILITY STATEMENT

DISTRIBUTION STATEMENT A: Approved for public release; distribution is unlimited.

13. SUPPLEMENTARY NOTES

14. ABSTRACT

Additive manufacturing (AM), otherwise known as 3D printing, is a growing research area for RF (radio frequency) components due to its low cost, lightweight, rapid manufacturing characteristics and its ability to easily fabricate complex designs. Dielectric printing is one area that has gathered increased interest in recent years for RF applications. With AM, dielectrics can easily be fabricated in complex and conformal shapes or bulk material properties can be modified by controlling the volume fill of the print. Lattice structures can be utilized to alter the ratio of air vs material to modify the bulk material properties. This report presents an analysis on material latticing and its effect of bulk dielectric properties to aid in AM dielectric design. .

15. SUBJECT TERMS

Additive manufacturing
Lattice printing
Material characterization

16. SECURITY CLASSIFICATION OF:			**17. LIMITATION OF ABSTRACT**	**18. NUMBER OF PAGES**	**19a. NAME OF RESPONSIBLE PERSON**
					Anna Stumme
a. REPORT	**b. ABSTRACT**	**c. THIS PAGE**	U	18	**19b. TELEPHONE NUMBER** *(include area code)*
U	U	U			(202) 404-3300

Standard Form 298 (Rev. 8-98)
Prescribed by ANSI Std. Z39.18

This page intentionally left blank.

CONTENTS

This page intentionally left blank.

FIGURES

This page intentionally left blank.

ANALYSIS OF BULK DIELECTRIC CONSTANT OF LATTICED MATERIALS

1. Introduction

Additive manufacturing (AM), otherwise known as 3D printing, is a growing research area for RF (radio frequency) components due to its low cost, lightweight, rapid manufacturing characteristics and its ability to easily fabricate complex designs. Dielectric printing is one area that has gathered increased interest in recent years for RF applications. With AM, dielectrics can easily be fabricated in complex and conformal shapes or bulk material properties can be modified by controlling the volume fill of the print. This has led to research in AM Luneburg lenses [1, 2] where space filling curves [3, 4], perforations [5], or lattice structures are utilized to control the ratio of material vs. air (the volume fill) to modify the bulk material properties, namely the bulk dielectric constant. This report presents an analysis on material latticing and its effect on bulk dielectric properties to aid in AM dielectric design.

2. Background

Much of this background discussion draws from [6] but it is important to repeat many of the details in that report for full understanding of the lattice study discussed in Section 3. However, [6] contains more details than provided in Section 2 and is a helpful reference for further discussion of the use and design of lattices.

2.1 Additive Manufacturing

Additive manufacturing is a broad term that encompasses fabrication methods which create a part through additive methods, building a part layer-by-layer. This is in contrast to subtractive manufacturing, otherwise known as traditional manufacturing, where parts are built by removing material until the desired part is achieved. Due to the additive method of fabrication, AM is capable of fabricating complex, abnormally shaped parts with relative ease that would be impossible, or at least immensely difficult, for subtractive manufacturing to achieve. This ability to utilize all of the 3 dimensional design space is one of the big draws for AM and is why it has become such an attractive manufacturing method.

AM is not a single fabrication process. Instead multiple AM processes exist, each fabricating parts in an additive manner but with different methods of building parts. The 7 main types of additive manufacturing are material extrusion, material jetting, binder jetting, vat photopolymerization, powder bed fusion, directed energy deposition, and sheet lamination. While the different AM processes are not critical to the lattice density analysis conducted and discussed in Section 3, it is important to note that the different AM processes will affect lattice selection due to the manufacturability concerns with different processes. However, manufacturability of lattices in different AM processes is outside the scope of this paper and will be analyzed in future work.

Manuscript approved April 14, 2023.

2.2 Lattices for AM

Lattice structures are repeated patterns that fill some part or space [7]. All lattice structures can be broken down to a unit cell which is the repeating structure in the lattice pattern, otherwise named the lattice type. There are several different types of lattices but for this study we will focus on triply periodic minimal surfaces (TPMS) and graph lattice types. Two variables control the unit cell of a lattice: unit cell size and thickness. As discussed in [6], the ratio between these two variables set the volume fill of a lattice and will be discussed more in Section 2.2.1. Since the term "unit cell" will be utilized in a different context in Section 3.2, for the rest of the report a lattice unit cell will only be referred to as lattice cell as to minimize ambiguity.

2.2.1 Designing Latticed Materials for Fill Volume

The previous work, presented in [6], analyzed 17 different lattice structures (shown in Appendix) and how the ratio between lattice cell size and thickness controlled each lattice's percent fill volume. Different lattices with the same cell size and thickness resulted in different percent fill volumes. In [6], lookup plots and tables were generated and presented to provide an easy method of designing a lattice for a particular percent fill volume. With the lookup table and plots a user can select a lattice type and fill percentage and determine the cell size to thickness ratio needed. This work will be utilized in Section 3 to simulate latticed materials at different percent fill to evaluate the relationship between percent fill and dielectric constant.

3. Latticing Effect on Material Properties

A parametric study was set up and run to evaluate how material properties change with lattice type and fill percentage. In Section 3.1 the calculations to extract the material's permittivity and permeability from S-Parameters are described. Section 3.2 details the simulation setup with the simulation study results and analysis is presented in Section 3.3

3.1 Calculating Material Properties

The material properties (permittivity, ε, and permeability, μ) of a material under test (MUT) can be determined from measured (or simulated) S-Parameters, when the is MUT excited by a plane wave. Such a simulation setup will be discussed and detailed in Section 3.2, while the common measurement methods include measuring dielectric in a waveguide [8] or coax [8] as well as free space systems [8–10]. Once the S-Parameter data is obtained the material properties can be calculated.

To begin, the impedance parameters (Z) are calculated from the S-parameters using (1), found in [11].

$$\begin{aligned} Z_{11} &= Z_0 \frac{(1+S_{11})(1-S_{22})+S_{12}S_{21}}{(1-S_{11})(1-S_{22})-S_{12}S_{21}} \\ Z_{12} &= Z_0 \frac{2S_{12}}{(1-S_{11})(1-S_{22})-S_{12}S_{21}} \\ Z_{21} &= Z_0 \frac{2S_{21}}{(1-S_{11})(1-S_{22})-S_{12}S_{21}} \\ Z_{22} &= Z_0 \frac{(1-S_{11})(1+S_{22})+S_{12}S_{21}}{(1-S_{11})(1-S_{22})-S_{12}S_{21}} \end{aligned} \tag{1}$$

Then the ABCD matrix can be calculated using (2), also found in [11].

$$\begin{aligned} A &= \frac{Z_{11}}{Z_{21}} \\ B &= \frac{Z_{11}Z_{22} - Z_{21}Z_{12}}{Z_{21}} \\ D &= \frac{Z_{22}}{Z_{21}} \\ Z_{Bloch} &= \frac{2B}{A - D + \sqrt{(A+D)^2 - 4}} \end{aligned} \tag{2}$$

With the impedance Z_{Bloch} from (2) the material parameters ε_r and μ_r can be found using (3) and (4). These material paramteter equations are obtained through knowing $Z = \sqrt{\mu/\varepsilon}$, $k = \omega\sqrt{\mu\varepsilon}$, and $\omega = 2\pi f$. The rest is equation substitution and solving for the relative permittivity (ε_r) and permeability (μ_r).

$$\varepsilon_r = \frac{k}{\varepsilon_0 2\pi f Z_{Bloch}} \tag{3}$$

$$\mu_r = \frac{k Z_{Bloch}}{\mu_0 2\pi f} \tag{4}$$

Through these sets of equations (1) - (4) the relative permittivity and permeability of a MUT can be found from the S-Parameters.

3.2 Simulation Setup

A simulation setup is needed that can obtain the S-Parameters of a plane wave exciting a MUT. This requires a sufficiently large sample of material to emulate a plane wave interacting with an infinite slab of finite thickness. However, for a latticed material this results in a large amount of lattice cells within the slab causing a significant increase in computation and run time required for a simulation due to the increased meshing required to accurately capture the lattice details. Instead, a unit cell approach can be taken to greatly reduce these computational requirements thus reducing the run time to simulate a MUT.

The unit cell setup is shown in Fig. 1 for a solid block of material. Instead of simulating a large slab of the material, a smaller block of material is set in the unit cell, Fig. 1(a), with the *z*-axis defining the direction of propagation for normal incidence with the MUT. The thickness of the MUT is measured along the *z*-axis. In the *x* and *y*-directions lattice pairs are defined on the unit cell walls, Fig. 1(c), to effectively simulate an infinite slab in those directions. For a solid block, like in Fig. 1, this simulates an infinite solid slab of material in *x* and *y* with the finite thickness in *z*. Two floquet ports are defined on the top and bottom of the unit cell, shown in Fig. 1(b), to simulate a plane wave through the material and to obtain the full 2 port S-Parameters needed to calculate the material parameters, detailed in Section 3.1. The floquet ports are de-embedded to the top and bottom face of the MUT, as indicated by the arrows from the port to the MUT. To validate the unit cell method the model in Fig. 1(a), with the material block defined as teflon, was run and S-Parameters extracted. The dielectric constant, or relative permittivity (ε_r), was calculated using the equations in Section 3.1 and the results, Fig. 2, show excellent agreement with the relative permittivity of teflon, $\varepsilon_{teflon} = 2.1$.

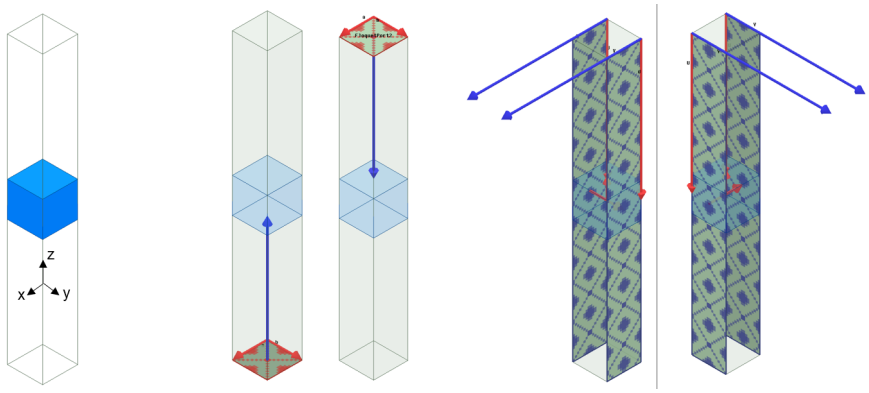

(a) Unit Cell (b) Floquet Ports (c) Lattice Pair Definition

Fig. 1 — Unit cell simulation setup

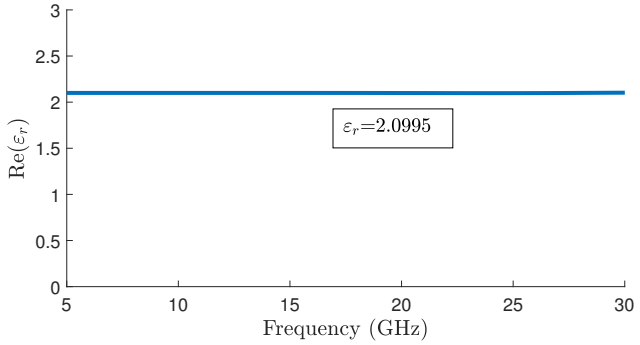

Fig. 2 — Calculated dielectric constant from unit cell setup shown in Figure 1.

3.3 Lattice Study and Results

With the simulation method validated for a known block of material the simulation method can be used to investigate the effect of using latticed materials. The setup is similar to that of Fig. 1, except of instead of a solid block of material a lattice cell of material is placed in the unit cell. This effectively simulates a latticed material with finite thickness in the z-direction and infinite latticed material in the x and y directions, more specifically an infinitely repeating lattice cell in those directions.

A latticed material should effectively change the bulk dielectric constant of the material through the introduction of air in the material. Since the material and air have different dielectric constants the overall bulk dielectric constant the plane wave interacts with changes. It would seem intuitive that the new bulk dielectric constant should be the volume weighted average of the dielectric constants of the latticed material and air. With this method, the effective bulk dielectric constant (ε_{eff}) is calculated using (5), where f_{mat} is the volume fraction of material to air, f_{air} the volume fraction of air (with $f_{air} = 1 - f_{mat}$), ε_{mat} the

dielectric constant of the material, and ε_{air} the dielectric constant of air.

$$\varepsilon_{eff} = \frac{(f_{mat} * \varepsilon_{mat}) + (f_{air} * \varepsilon_{air})}{f_{mat} + f} \tag{5}$$

However, other effective bulk dielectric estimation methods exist, like the Bruggeman [12] and Maxwell Garnett [12] methods.

$$\begin{aligned} H_{brugg} &= (3f_{mat} - 1)\varepsilon_{mat} + (3f_{air} - 1)\varepsilon_{air} \\ \varepsilon_{eff} &= \frac{H_{brugg} + \sqrt{H_{brugg}^2 + 8\varepsilon_{mat}\varepsilon_{air}}}{4} \end{aligned} \tag{6}$$

The Bruggeman method uses (6) where the Maxwell Garnett method uses (7) to calculate the effective bulk dielectric constant, ε_{eff}.

$$\varepsilon_{eff} = \varepsilon_{mat} + f_b(\varepsilon_{air} - \varepsilon_{mat})\frac{3\varepsilon_{mat}}{3\varepsilon_{mat} + (1 - f_{mat})(\varepsilon_{air} - \varepsilon_{mat})} \tag{7}$$

These approximation methods will be evaluated against the simulated lattices to evaluate their accuracy for lattices.

The simulation study involved running each of the lattices from [6] at a percent fill of 10 to 80% in 10% increments. This study was set up as such to evaluate if lattice type has any affect on the bulk dielectric constant as well as evaluating the approximation methods. From the simulation results, Fig. 3, the bulk dielectric constants calculated for the difference lattice types agree fairly well across the varying fill volume. In Fig. 4, the overall spread of the calculated dielectric constant for the lattices is shown. The largest variation between the highest calculated dielectric constant of a lattice vs. the lowest calculated dielectric constant is, found with $|max(\varepsilon_{lattices}) - min(\varepsilon_{lattices})|$, is 0.045. However, the comparison between the

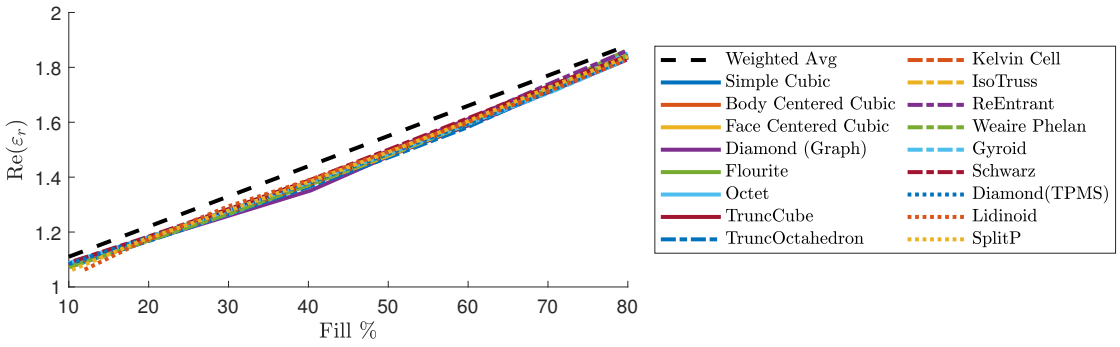

Fig. 3 — Results of lattice simulation study, compared to weighted average approximation.

calculated dielectric constant and the dielectric approximations, Fig. 5, have some variations. The weighted average approximation is the least correlated to the simulated bulk dielectric constant. The Maxwell Garnett

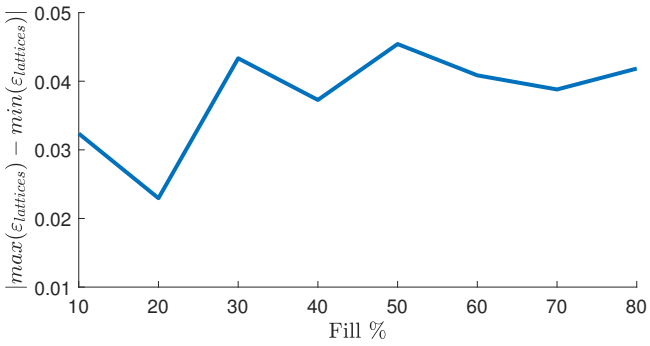

Fig. 4 — Maximum difference in calculated dielctric constant for all lattices.

approximation shows fairly good agreement however, the Bruggeman approximation is in the best agreement to the simulated bulk dielectric constant for the lattices run. To compare the approximations (8) is used to show the difference between the simulated dielectric constant, $\varepsilon_{lattice}$, and an approximated bulk dielectric constant ε_{approx}.

$$\Delta \equiv |\varepsilon_{lattice} - \varepsilon_{approx}| \tag{8}$$

This is demonstrated in Fig. 6 with Bruggeman approximation the lowest Δ across the fill study, Maxwell Garnett approximation with a slightly higher Δ for the larger fill percentages and the weighted average with the largest Δ for all the fill percentages evaluated, as compared to a single lattice type - Simple Cubic. Similar comparisons for the rest of the lattice types can be found in the Appendix. This indicates that the

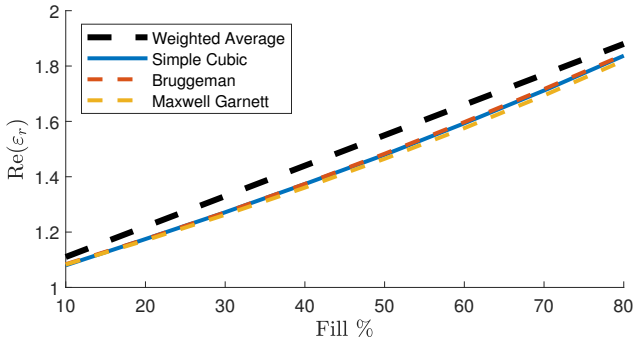

Fig. 5 — Comparison between simple cubic lattice simulation results and the three dielectric constant approximation methods.

Bruggeman approximation is a good approximation method to utilize for designing dielectrics with latticed materials.

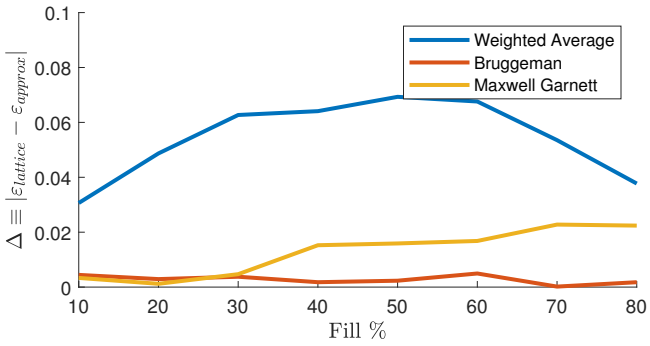

Fig. 6 — Difference between simulated dielectric constant results for simple cubic lattice and the three dielectric constant approximation methods.

4. Summary

A simulation study was performed to analyze the effect of material latticing on bulk dielectric properties of a material. While the lattices showed good agreement with each other across different fill volumes the dielectric approximation methods showed some variation from simulated results. The closest approximation method was the Bruggeman approximation indicating it is a viable approximation method to estimate the bulk dielectric constant of latticed materials.

5. Future Work

While this study indicated that lattice type has little effect of the bulk dielectric constant of a material, this will need to be re-evaluated for different material types and unit cell sizes to ensure this relationship doesn't break down outside of this study's setup.

Appendix A

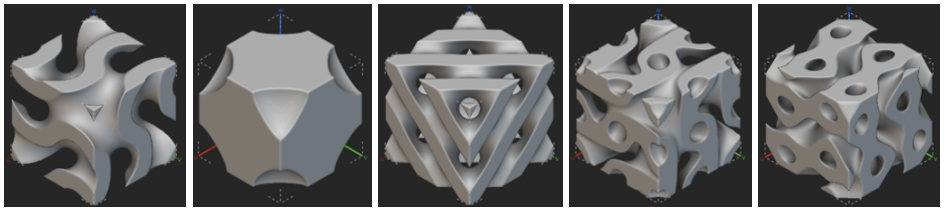

(a) Gyroid (b) Schwarz (c) Diamond (d) Lidinoid (e) SplitP

Fig. A1 — TPMS unit cells.

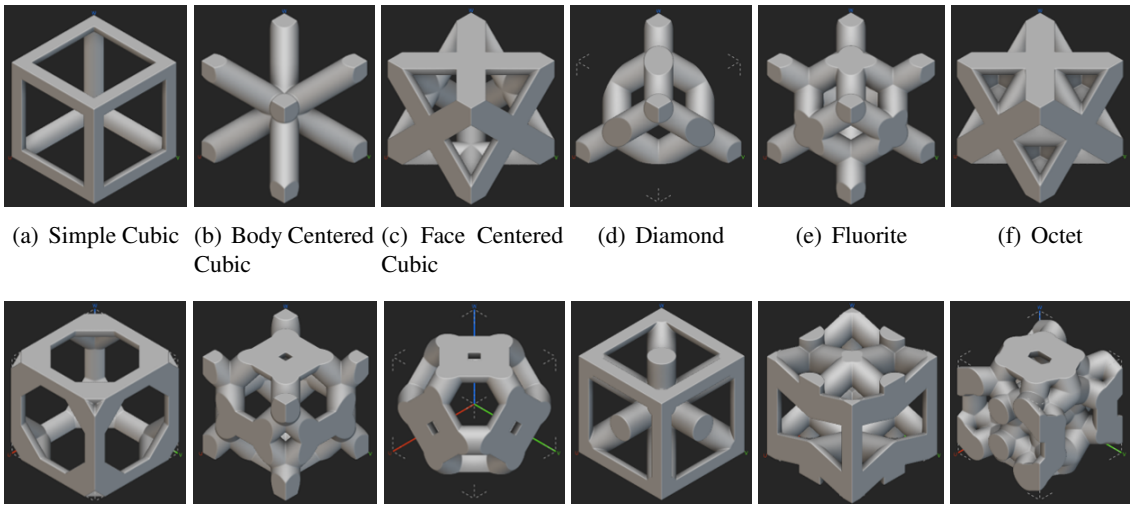

(a) Simple Cubic (b) Body Centered Cubic (c) Face Centered Cubic (d) Diamond (e) Fluorite (f) Octet

(g) Truncated Cube (h) Truncated Octahedron (i) Kelvin Cell (j) IsoTruss (k) Re-Entrant (l) Weaire-Phelan

Fig. A2 — Graph unit cells.

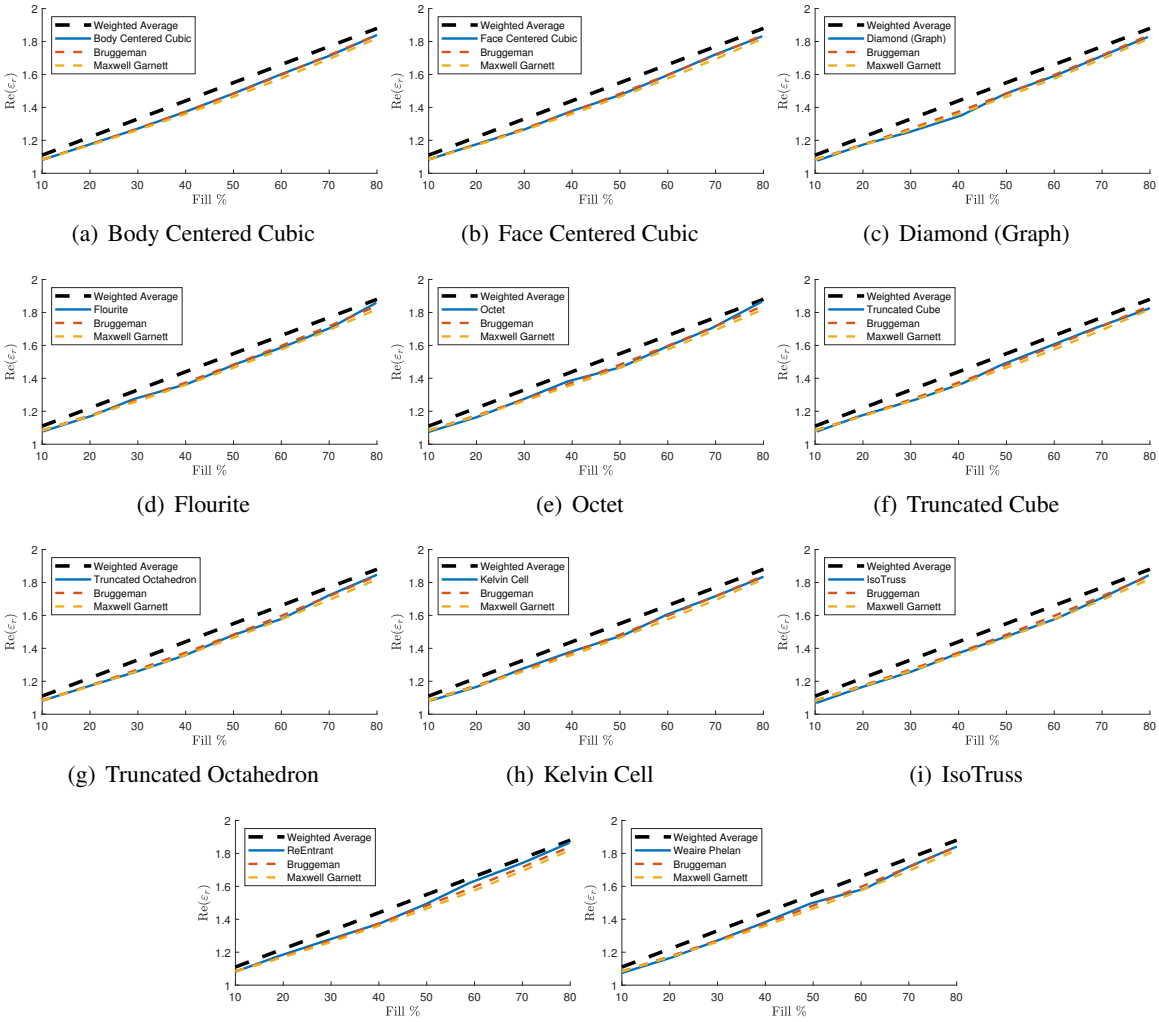

(a) Body Centered Cubic (b) Face Centered Cubic (c) Diamond (Graph)

(d) Flourite (e) Octet (f) Truncated Cube

(g) Truncated Octahedron (h) Kelvin Cell (i) IsoTruss

(j) Re-Entrant (k) Weaire Phelan

Fig. A3 — Comparisons between the rest of the graph lattice type simulation results and the three dielectric constant approximation methods.

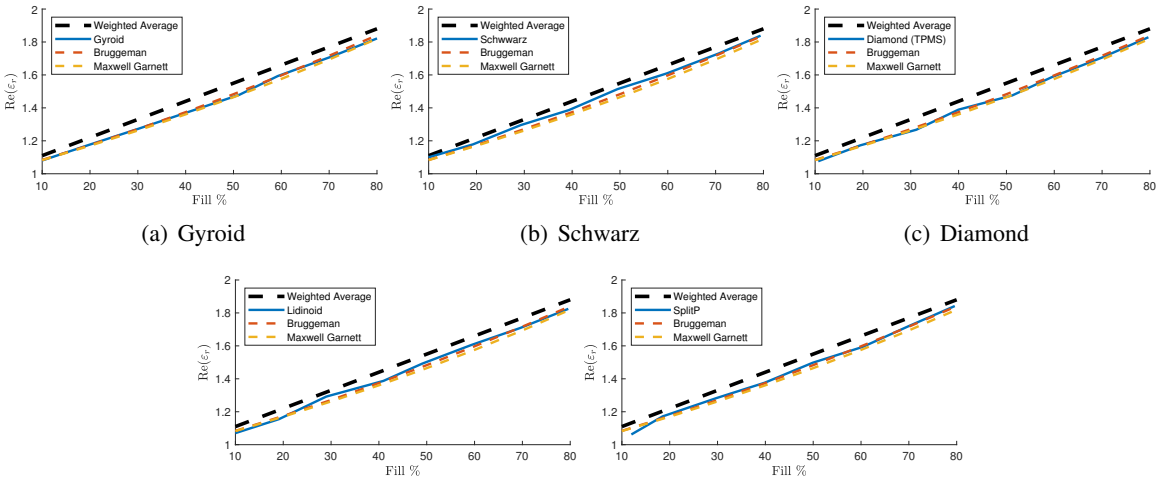

(a) Gyroid (b) Schwarz (c) Diamond

(d) Lidinoid (e) Split P

Fig. A4 — Comparisons between the TPMS lattice type simulation results and the three dielectric constant approximation methods.

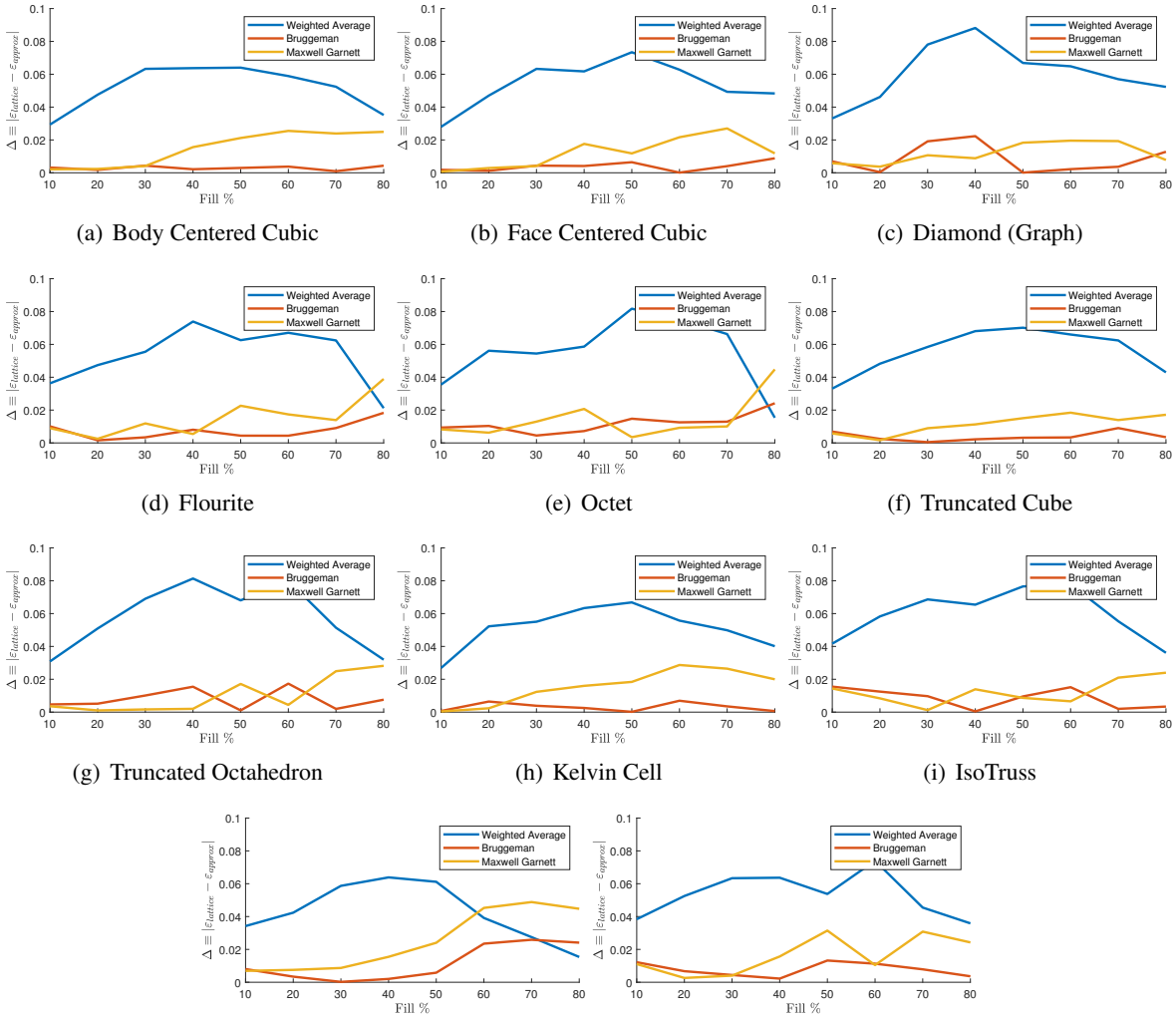

(a) Body Centered Cubic (b) Face Centered Cubic (c) Diamond (Graph)

(d) Flourite (e) Octet (f) Truncated Cube

(g) Truncated Octahedron (h) Kelvin Cell (i) IsoTruss

(j) Re-Entrant (k) Weaire Phelan

Fig. A5 — Difference between simulated dielectric constant results for the rest of the graph lattice types and the three dielectric constant approximation methods.

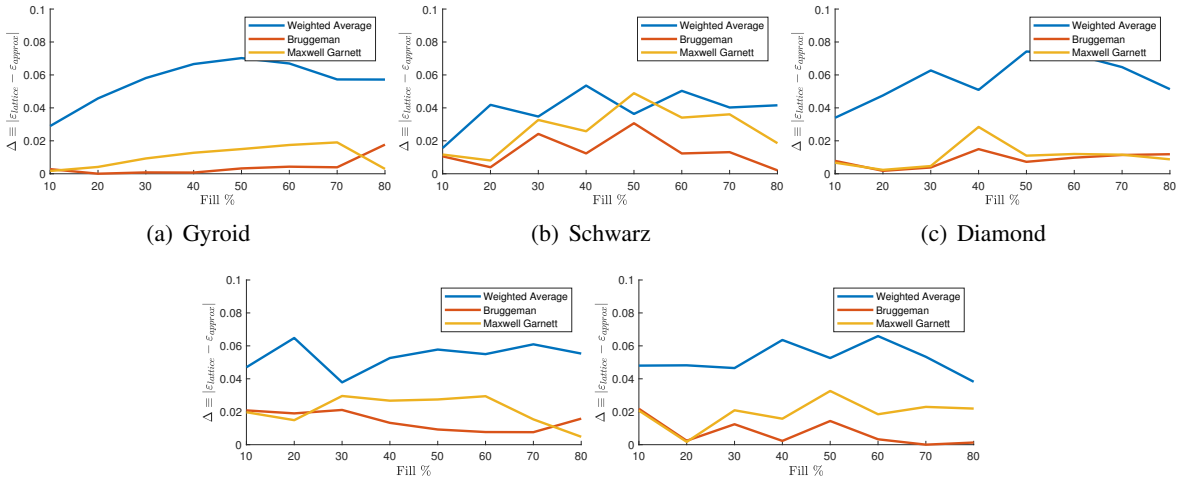

(a) Gyroid (b) Schwarz (c) Diamond

(d) Lidinoid (e) Split P

Fig. A6 — Difference between simulated dielectric constant results for the TPMS lattice types and the three dielectric constant approximation methods.

REFERENCES

[1]I. Grigoriev, I. Munina, and D. Zelenchuk, "Design aspects of 3d printing for gradient index lenses," in *2022 16th European Conference on Antennas and Propagation (EuCAP)*, 2022, pp. 1–4.

[2]M. AlMansoori, A. Rangel, J. Pantoja, F. Vega, A. Banelli, C. Kasmi, L. O. Fichte, and M. Stiemer, "A study of materials and additive manufacturing techniques for a novel 2d luneburg lens," in *2022 IEEE International Symposium on Antennas and Propagation and USNC-URSI Radio Science Meeting (AP-S/URSI)*, 2022, pp. 1594–1595.

[3]Z. Larimore, S. Jensen, A. Good, A. Lu, J. Suarez, and M. Mirotznik, "Additive manufacturing of luneburg lens antennas using space-filling curves and fused filament fabrication," *IEEE Transactions on Antennas and Propagation*, vol. 66, no. 6, pp. 2818–2827, 2018.

[4]Z. Larimore, S. Jensen, P. Parsons, B. Good, K. Smith, and M. Mirotznik, "Use of space-filling curves for additive manufacturing of three dimensionally varying graded dielectric structures using fused deposition modeling," *Additive Manufacturing*, vol. 15, pp. 48–56, 2017. [Online]. Available: https://www.sciencedirect.com/science/article/pii/S2214860416301683

[5]P. Kadera and J. Lacik, "Performance comparison of w-band luneburg lens antenna: Additive versus subtractive manufacturing," in *2021 20th International Conference on Microwave Techniques (COMITE)*, 2021, pp. 1–6.

[6]A. Stumme, M. Dorsey, and A. Golding, "Analysis of lattice unit cells for additive manufacturing," Naval Research Laboratory, Washington, DC, Tech. Rep. NRL/IR/5317/23/1/U, January 2023.

[7]A. B. Varotsis. (2022) Guide to lattice structures in additive manufacturing. https://ntopology.com/blog/guide-to-lattice-structures-in-additive-manufacturing/.

[8]R. A. Fenner, E. J. Rothwell, and L. L. Frasch, "A comprehensive analysis of free-space and guided-wave techniques for extracting the permeability and permittivity of materials using reflection-only measurements," *Radio Science*, vol. 47, no. 01, pp. 1–13, 2012.

[9]N. Zhang, J. Cheng, P. Gong, and H. Ma, "A broadband free-space dielectric measurement system," in *2015 IEEE MTT-S International Microwave Workshop Series on Advanced Materials and Processes for RF and THz Applications (IMWS-AMP)*, 2015, pp. 1–3.

[10]D. Ghodgaonkar, V. Varadan, and V. Varadan, "A free-space method for measurement of dielectric constants and loss tangents at microwave frequencies," *IEEE Transactions on Instrumentation and Measurement*, vol. 38, no. 3, pp. 789–793, 1989.

[11]D. M. Pozar, *Microwave engineering; 3rd ed.* Hoboken, NJ: Wiley, 2005. [Online]. Available: https://cds.cern.ch/record/882338

[12]J. Humlicek, *Data Analysis for Nanomaterials: Effective Medium Approximation, Its Limits and Implementations*, 03 2013, pp. 145–178.